Electronic Supplementary Material (ESI) for Lab on a Chip.

Supplementary materials for

Diffusiophoretic Exclusion of Colloidal Particles for Continuous Water Purification

Hyomin Lee, Junsuk Kim, Jina Yang, Sang Woo Seo and Sung Jae Kim

Supplementary Note 1. Comparison of fully-coupled and simplified model.

The comparisons of the fully-coupled model (equation (14) – (18) in main text) and simplified model (equation (1) – (3) in main text) were plotted in Supplementary Figure 1. The errors between two models were negligible.

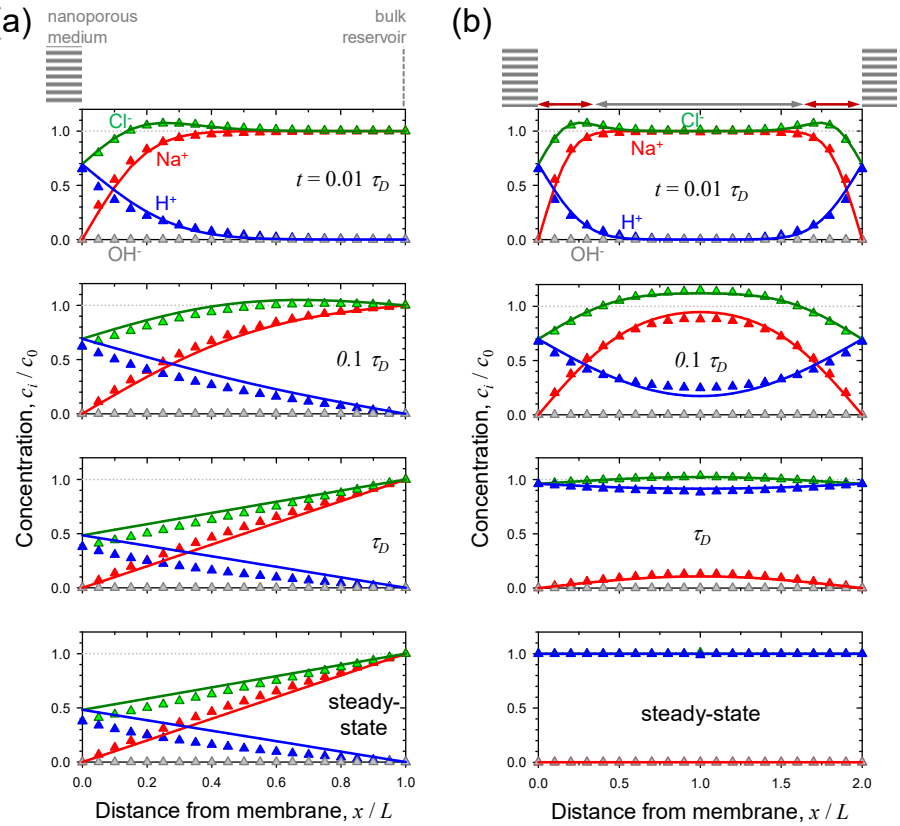

Supplementary Figure 1. Fully-coupled model vs. simplified model. Concentration profiles for (a) porous medium / electrolyte and (b) porous medium / electrolyte / porous medium system. Symbols (▲) and solid lines were obtained from the fully-coupled and the simplified model, respectively. The errors between two models were negligible.

Supplementary Note 2. Scaling analysis and non-dimensionalization for boundary layer.

Through the simplification of fully-coupled model, the steady-state mass conservation of Na^+ was described as

$$D_{eff}\frac{\partial^2 c_{Na}}{\partial x^2}+D_{eff}\frac{\partial^2 c_{Na}}{\partial y^2}-\frac{\partial}{\partial y}\left(c_{Na}u_y\right)=0 \tag{S1}$$

where x and y are the spatial coordinates and u_y is the y-component of flow field. Each term of above equation was scaled as

$$O\left(\frac{D_{eff}c_0}{W^2}\right)+O\left(\frac{D_{eff}c_0}{L_n{}^2}\right)-O\left(\frac{c_0U_{mean}}{L_n{}^2}\right)=0 \tag{S2}$$

where W is the half-width of the microchannel, L_n is the length of the nanoporous medium as depicted in Supplementary Figure 2 and U_{mean} is the mean velocity of the introduced flow. Typically, $W << L$ so that

$$O\left(\frac{D_{eff}c_0}{W^2}\right)>>O\left(\frac{D_{eff}c_0}{L_n{}^2}\right). \tag{S3}$$

This means that the second term in equation (S3) can be neglected. Thus,

$$D_{eff}\frac{\partial^2 c_{Na}}{\partial x^2}-\frac{\partial}{\partial y}\left(c_{Na}u_y\right)\approx 0\,. \tag{S4}$$

By selecting characteristic scales (c_0 for c_{Na}, W for x, L_n for y and U_{mean} for u_y), the dimensionless form of equation (S4) was

$$\frac{\partial^2 \tilde{c}_{Na}}{\partial \tilde{x}^2}-Sh\frac{\partial}{\partial \tilde{y}}\left(\tilde{c}_{Na}\tilde{u}_y\right)=0 \tag{S5}$$

where '~' means dimensionless variables and Sh is the Sherwood number. The definition of Sh was

$$Sh=\frac{W^2U_{mean}}{L_nD_{eff}} \tag{S6}$$

which means the ratio of longitudinal convective transfer and transverse diffusion rate.

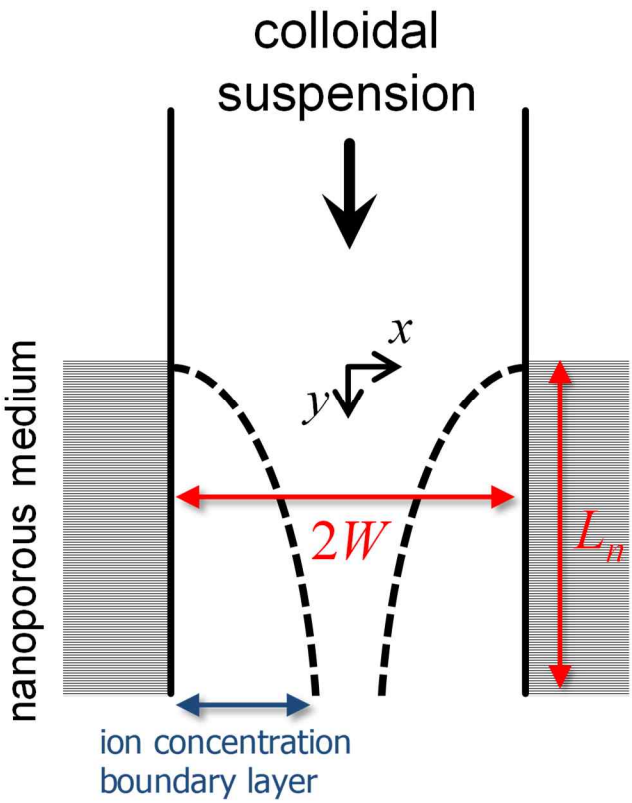

Supplementary Figure 2. Domain descriptions for scaling analysis.

Supplementary Note 3. Effect of finite internal H^+ inside ion exchange medium.

In main text, we assumed infinite amount of H^+ ions in ion exchange materials to analyze the diffusiophoretic migration. However, in actual case, the H^+ is finite so that the diffusiophoretic exclusion is impermanent. Based on our previous measurement [1], we figured out that the Donnan concentration of Nafion was equivalent to the electrolyte concentration of ~1.4 M. This value means the initial amount of H^+ inside the Nafion is approximately 1.4 M. Utilizing the numerical model presented in below, we tracked the concentration change due to the finite H^+ ions (1.4 M) when 1 mM NaCl was exchanged.

Under porous medium / electrolyte domain as one-dimensional system depicted in Supplementary Figure 4(a), the transport phenomena of charged species (Na^+, H^+, Cl^- and OH^-) were described by the Nernst-Planck equations.

$$\frac{\partial c_i}{\partial t} = -\frac{\partial}{\partial x}\left(-D_i \frac{\partial c_i}{\partial x} - \frac{z_i F D_i}{RT} c_i \frac{\partial \psi}{\partial x} \right) + R_i \tag{S7}$$

where c_i is the concentration of i-th species, t is the time, x is the spatial coordinate, D_i is the diffusivity of i-th species, z_i is the ionic valence, F is the Faraday constant, R is the gas constant, T is the absolute temperature, ψ is the electric potential and R_i is the reaction rate of i-th species. For Na^+ and Cl^-, R_i became zero because they were inert species to chemical reactions. However, for H^+ and OH^-, they react each other such as $H^+ + OH^- \leftrightarrow H_2O$ which is water self-ionization. Thus, R_H and R_{OH} were represented by $k_{rxn}(K_w - c_H c_{OH})$ where k_{rxn} is the reaction rate constant and K_w is the equilibrium of the self-ionization. The electrical interaction between each ionic species can be obtained from the Poisson equation. For the electrolyte domain (right side of Supplementary Figure 4(a)),

$$-\varepsilon \nabla^2 \psi = F\left(c_{Na} - c_{Cl} + c_H - c_{OH}\right) \tag{S8}$$

where ε is the electrical permittivity of water. On the other hands, following Poisson equation

should be needed for the cation-selective domain (left side of Supplementary Figure 4(a)).

$$-\varepsilon\nabla^2\psi = F\left(c_{Na} - c_{Cl} + c_H - c_{OH} - N\right) \tag{S9}$$

where N is the Donnan concentration of the medium. If the medium has extremely low water permeability, the effect of flow field on the ionic transportation can be neglected in the 1D system. The boundary conditions at the bulk (right end of Supplementary Figure 4(a)) were that the concentration of each ionic species was set to be its bulk concentration ($c_{Na} = c_{Cl} = c_0$ and $c_H = c_{OH} = 10^3$ x $10^{-\mathrm{pH}}$ where c_0 is the specific bulk concentration and pH was assumed to 7 in this work) and the electric potential was zero. At the end of the medium (left end of Supplementary Figure 4(a)), all ionic fluxes became zero (physically no-penetration for mass) and zero-electric field was imposed (electrically no-penetration). Note that the fully-coupled model in the main text only considered the electrolyte domain. The initial conditions on electrolyte domain were $c_{Na} = c_{Cl} = c_0$, $c_H = c_{OH} = 10^3$ x $10^{-\mathrm{pH}}$ and zero electrical potential. On the other hand, inside the porous medium, the initial conditions were $c_{Na} = c_{Cl} = c_{OH} = 0$, $c_H = N$ and $\psi = -(RT/F)\ln(N/c_0)$ where these values can be determined by the Donnan equilibrium[2].

We conducted finite element simulations using commercial software (COMSOL Multiphysics 4.4, COMSOL Inc.) through above 1D formulations. Assuming that the boundary layer thickness in electrolyte side was $(3/Sh)^{1/3}$ x W (this scale was obtained from boundary layer analysis in main text) and exchange medium thickness (W_n) was 1.5 mm, Supplementary Figure 4(b) and 4(c) showed the minimum Na^+ concentration outside the ion exchange medium and remaining H^+ concentration inside the medium, respectively. The curves implied that the internal H^+ was totally exhausted over $O(10^4 \tau_D)$ so that the Na^+ concentration was recovered to its bulk concentration. All of the actual experiments lasted within this time confirming the results in this work were reliable. If the actual micro/nanofluidic ion exchange device has ~250

μm of W, the diffusion time (τ_D) is 37.65 s. Hence, when Sh = 10, the termination time of ion exchange is about 104.6 hours. The all experiments in this work were measured at 5 – 200 minutes (*i.e.* $8\,\tau_D$ – $320\,\tau_D$) so that the effect of finite H^+ was negligible. The simulation results denoted in Figure 6(a) and (b) in main text were evaluated at time below τ_D / Sh (= τ_U) and τ_D, respectively.

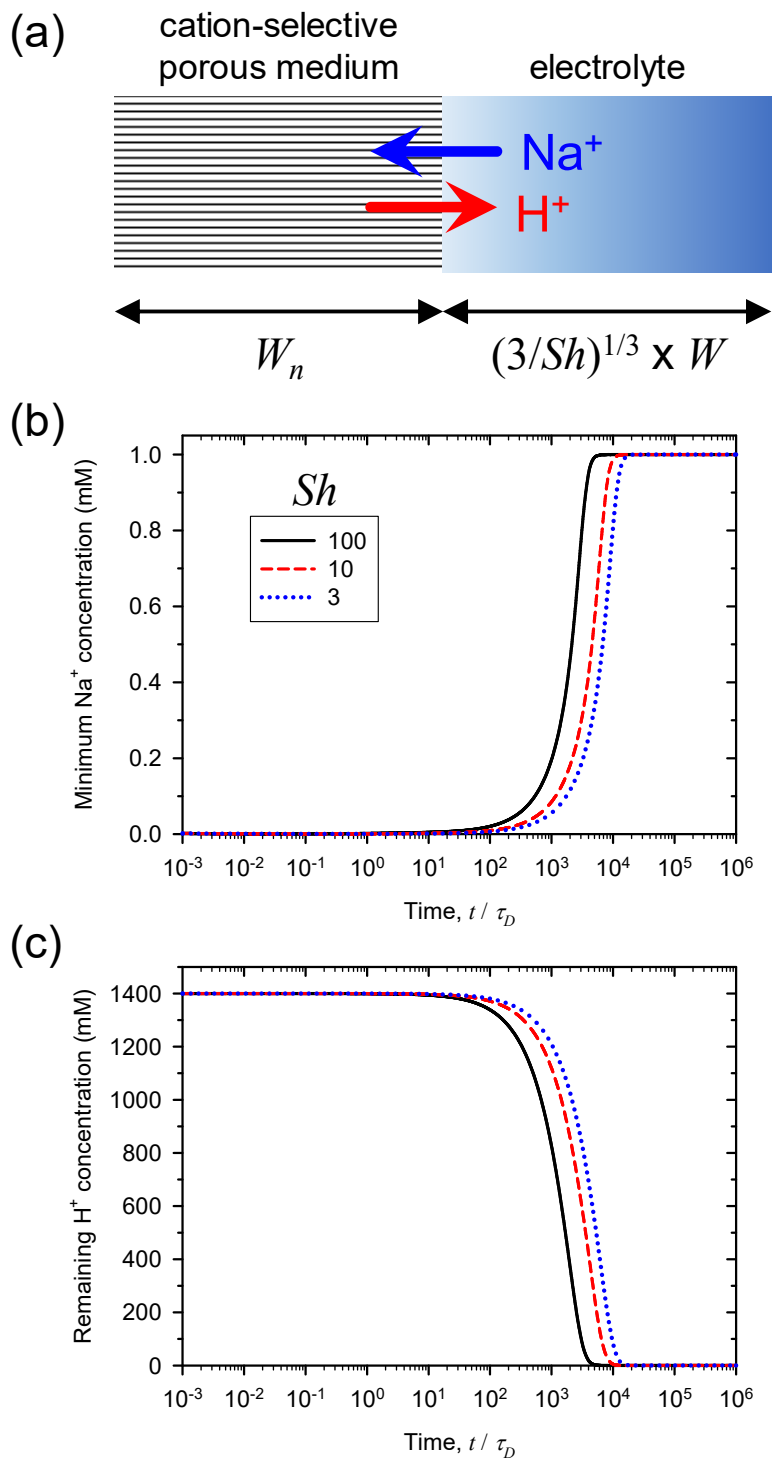

Supplementary Figure 3. Ion exchange with finite internal H^+. (a) Numerical domain description. (b) Minimum Na^+ concentration outside the cation-selective porous medium and (c) Remaining H^+ concentration inside the medium.

Supplementary Note 4. Diffusiophoretic exclusion of artificial microsphere with various *Sh*.

As shown in the below figure, the exclusion layer was directly visualized with various *Sh*. As *Sh* increased, the exclusion layer became thinner. See Supplementary Video2.

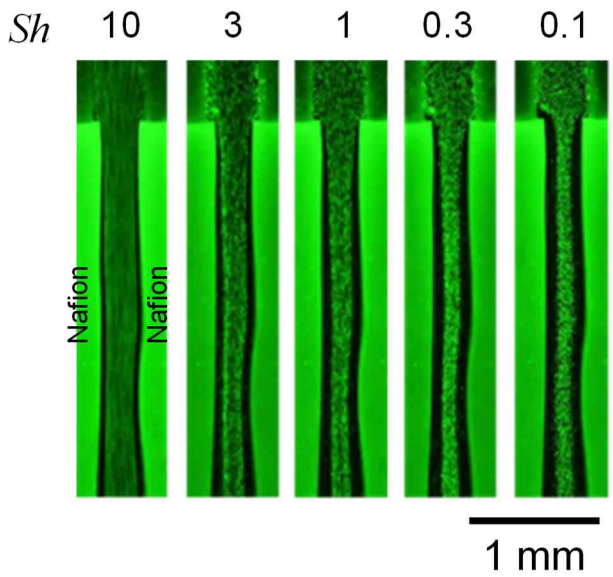

Supplementary Figure 4. Exclusion layer depending on *Sh*.

Supplementary Note 5. Sustainable time scale of diffusiophoretic exclusion.

The ion exchange process and diffusiophoretic exclusion were impermanent. The process stopped after all the interior protons were consumed. As discussed in main text, the scaling law of the exchange flux of Na^+ with respect to *Sh* was obtained by numerical simulation as shown in Supplementary Figure 5.

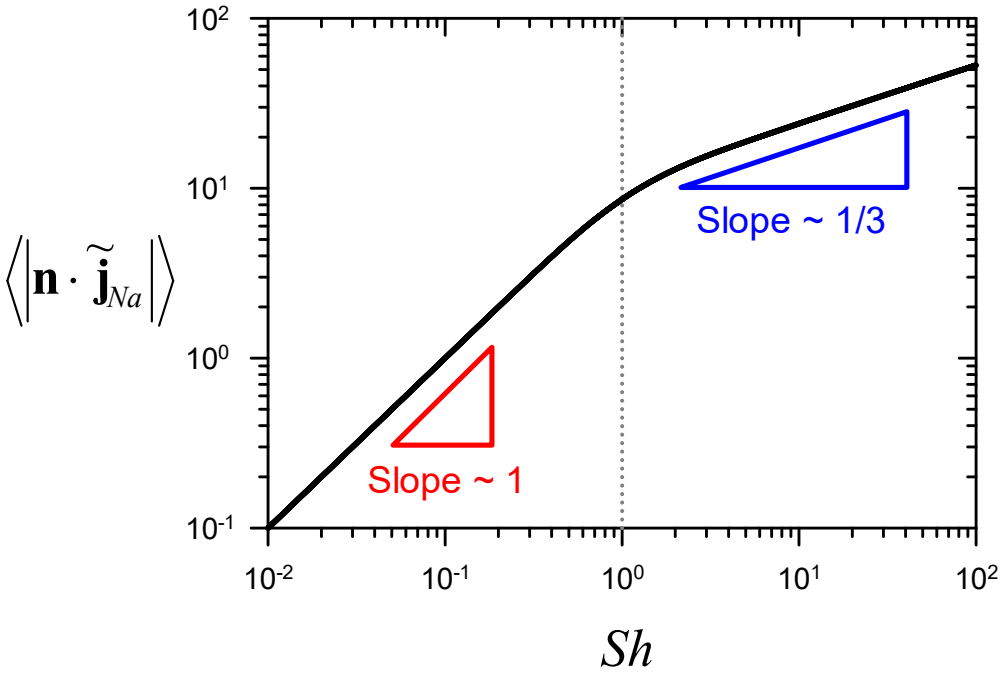

Supplementary Figure 5. Na^+ flux through the nanoporous medium as a function of *Sh*.

Supplementary Note 6. Long-time ion exchange to obtain actual sustainable time.

The equation (12) in main text implied the approximated sustainable time of our ion exchange device. In order to obtain the actual sustainable time, additional long-time experiment was conducted with 10 mM NaCl and Sh = 10 as shown in Supplementary Figure 6(a). The thickness of the exclusion layer was measured at ~2.3 mm from the starting point of Nafion after injection flow reached the steady state (~10 minutes). Negligible swelling and shrinking of Nafion were observed in the long-time operation. Adherence of colloidal particles to the glass substrate and photo bleaching of Nafion sheets were observed during the experiment. Asymmetric exclusion layers at each time were caused by leakage flow through the gap of Nafion/PDMS or Nafion/glass. However, the asymmetry was not critical to measure the layer thickness as a function of time. See Supplementary Video3 for more information. The exclusion layer was quantitatively measured in 5 different devices as shown in Supplementary Figure 6(b). The exclusion phenomenon was actually sustained over 8 hours. By linear extrapolation, the exclusion would be terminated after 18 hours, leading to

$$\frac{\tau_{sustain}}{\tau_D} = 5.31 \frac{N}{c_0} \frac{W_n}{W} \frac{1}{Sh^{1/3}} \tag{S10}$$

with N = 1,400 mol/m^3 based on our previous measurement [1], c_0 = 10 mol/m^3, W_n = 1.5 x 10^{-3} m, W = 2 x 10^{-4} m, Sh = 10 and τ_D = 25 s. Comparing to equation (12) in main text, the proportional parameter was ~5.31.

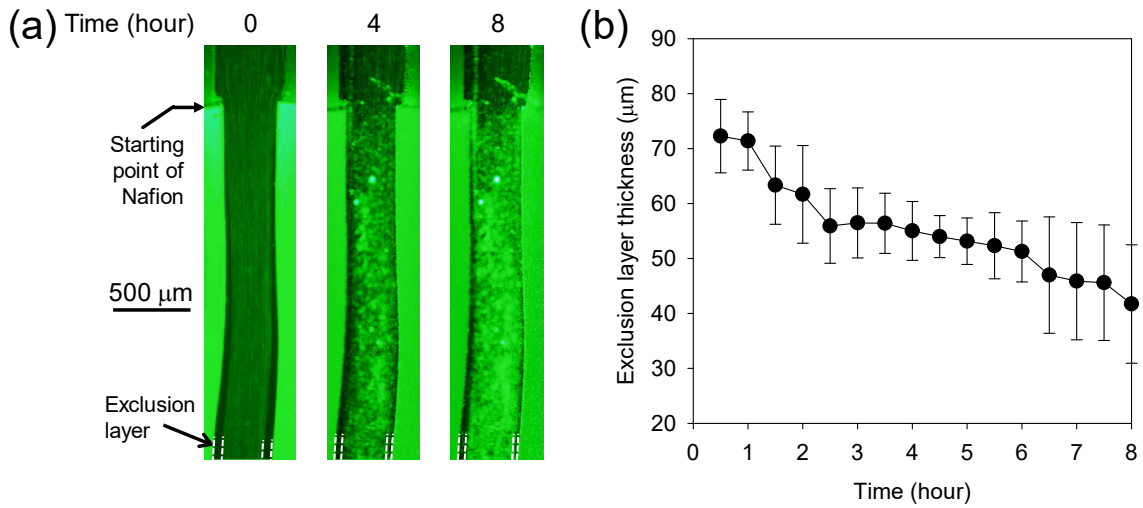

Supplementary Figure 6. Long-time operation on micro/nanofluidic ion exchange device. (a) Time-revolving snapshots of exclusion layer and (b) the thickness of exclusion layer as a function of time.

Supplementary Note 7. Numerical demonstration of zero Na+ concentration at the interface of cation-exchange medium and electrolyte.

The numerical formulations were described in Supplementary Note 3 whose domain was depicted in Supplementary Figure 7(a). As shown in Supplementary Figure 7(b), concentration profiles of each ionic species were obtained when N was equal to $10^3 \times c_0$. Supplementary Figure 7(c) showed the total ionic strength which was defined as $(c_{Na} + c_{Cl} + c_H + c_{OH}) / 2$. The profile of ionic strength implied that the effective total ion concentration spontaneously decreased by the ion exchange and the ion diffusion as we discussed in main text. In order to verify that the ion exchange led to the zero-concentration of non-protonic cation at the interface of EDL and diffuse layer, we investigated the cases of various N. When $N >> c_0$, the porous medium has a permselectivity (*i.e.* $\mathbf{j}_{Na} >> \mathbf{j}_{Cl}$ and $\mathbf{j}_{OH}$ where $\mathbf{j}_{Na}$, $\mathbf{j}_{Cl}$ and $\mathbf{j}_{OH}$ are ionic fluxes of Na^+, Cl^- and OH^- through the porous medium, respectively). As $N \rightarrow \infty$, the ideal permselectivity is guaranteed (*i.e.* $\mathbf{j}_{Cl}$, $\mathbf{j}_{OH}$ becomes zero). Supplementary Figure 7(d) showed that the Na^+ concentration at the interface became zero as N increased.

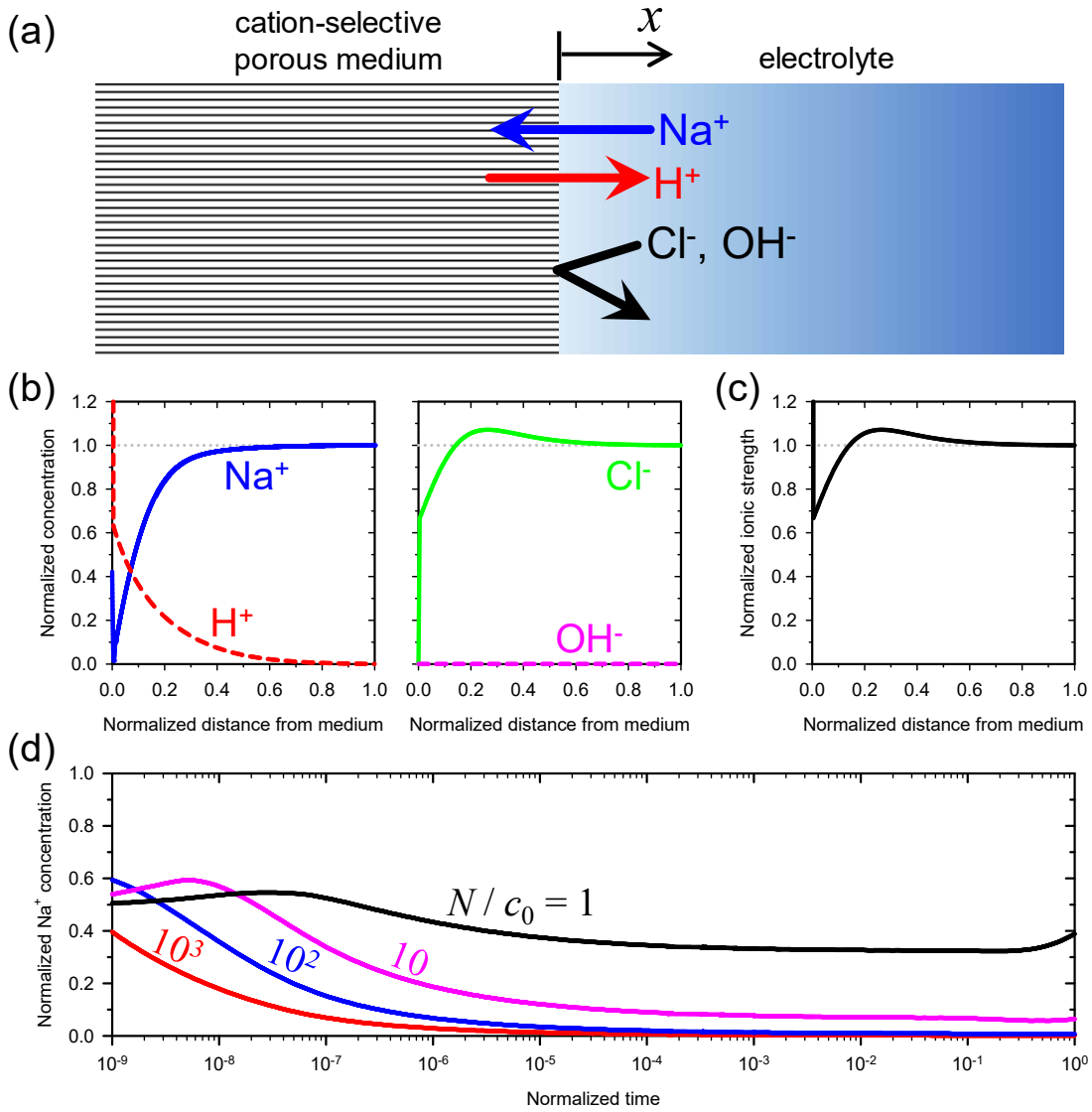

Supplementary Figure 7. Numerical analysis for permselective medium / electrolyte domain. (a) Domain description. Na^+ was exchanged with H^+. Due to the cation-selectivity, any anions were impermeable through the porous medium. (b) Concentration profiles when $N / c_0 = 10^3$ and $t / \tau_D = 0.01$. τ_D is the diffusion time scale which is defined as L^2 / D where L is the distance from the medium surface to bulk and D is the characteristic diffusivity. We chose the Na^+ diffusivity as D. The ion concentration of each ionic species was normalized by the bulk concentration of Na^+. (c) Total ionic strength normalized by the bulk concentration of Na^+. (d) Na^+ concentration at the interface of EDL and diffuse layer. The concentration and the time were normalized by the bulk concentration of Na^+ and the diffusion time scale.

Supplementary Note 8. Boundary conditions for 2D fully-coupled model.

Although we mentioned the boundary conditions for the 2D fully-coupled model to describe the ion concentration boundary layer in the main text, the summarized conditions presented for better understanding as shown in Supplementary Figure 8.

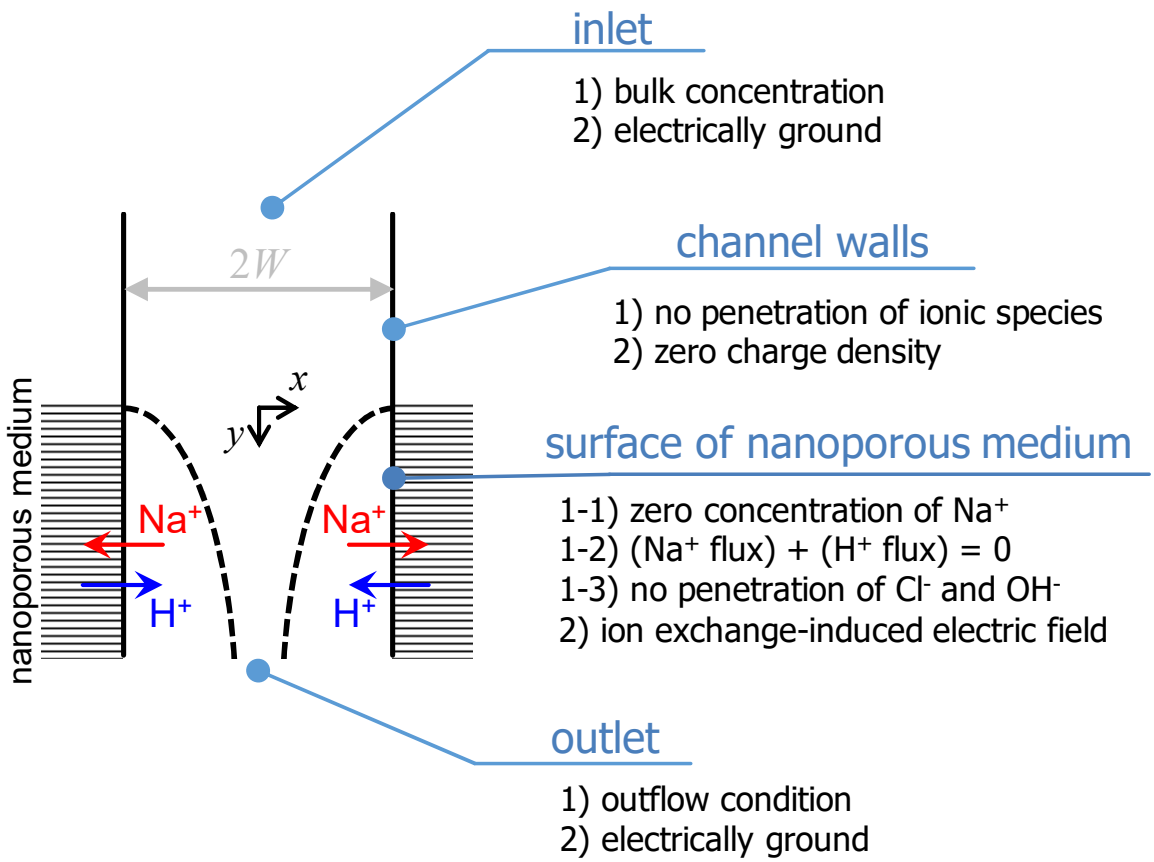

Supplementary Figure 8. Graphical representation of boundary conditions.

Supplementary Note 9. Diffusiophoresis in multiple-species electrolyte.

When a charged particle is immersed in an electrolyte-gradient environment, the particle propels along the concentration gradient. This motion has been called as diffusiophoresis. From several literatures [3-7], the particle propulsion velocity is represented by i) chemiphoretic contribution and ii) electrophoretic contribution;

$$\mathbf{U}_{CP} = -\frac{2\varepsilon R^2 T^2}{\eta F^2} \ln\left(1 - \tanh^2 \frac{F\zeta_p}{4RT}\right) \nabla \ln c_\infty , \tag{S11}$$

$$\mathbf{U}_{EP} = \frac{D_+ - D_-}{D_+ + D_-} \frac{RT}{F} \frac{\varepsilon \zeta_p}{\eta} \nabla \ln c_\infty \tag{S12}$$

and

$$\mathbf{U}_{DP} = \mathbf{U}_{CP} + \mathbf{U}_{EP} \tag{S13}$$

where $\mathbf{U}_{CP}$, $\mathbf{U}_{EP}$ and $\mathbf{U}_{DP}$ are the chemiphoretic, electrophoretic and diffusiophoretic velocity, respectively, ε is the electric permittivity of electrolyte, R is the gas constant, T is the absolute temperature around particle, η is the electrolyte viscosity, F is the Faraday constant, ζ_p is the particle zeta potential and c_∞ is the bulk concentration. Above equations are valid only for the case of 1:1 binary electrolyte (*e.g.* NaCl, KCl, *etc*). Ion exchange process produces multi-species electrolyte. Thus, above equations should be generalized for the case of the multi-electrolyte system.

As shown in Supplementary Figure 9(a), the charged particle was immersed in electrolyte-gradient that is governed by multi-ionic species. Assuming that there were n-kinds of monovalent ionic species, volumetric charge concentration (ρ_e) around the particle were represented as

$$\rho_e = F\sum_{i=1}^{n} z_i c_i \tag{S14}$$

where z_i and c_i are the valence and concentration of i-th species. Assuming monovalent electrolyte, z_i becomes +1 or -1. If $|\nabla c_{i\infty}| << \lambda_D^{-1}$ where λ_D is the Debye length, c_i can be represented by the Boltzmann distribution [5].

$$c_i = c_{i\infty} \exp\left(-\frac{z_i F\psi}{RT}\right) \tag{S15}$$

where ψ is the electric potential due to the electric double layer. Therefore, equation (S14) became

$$\rho_e = F\sum_{i=1}^{n} z_i c_{i\infty} \exp\left(-\frac{z_i F\psi}{RT}\right). \tag{S16}$$

If there were n^+-kinds of cationic species,

$$\rho_e = F\left[\sum_{i=1}^{n^+} c_{i\infty} \exp\left(-\frac{F\psi}{RT}\right) - \sum_{i=n^++1}^{n} c_{i\infty} \exp\left(\frac{F\psi}{RT}\right)\right] \tag{S17}$$

where first and second terms in bracket of right hand side represent the volumetric charge concentration due to cationic and anionic species, respectively. The multiple electrolyte should be satisfied with electroneutrality at the region far away from the particle. Mathematically,

$$\sum_{i=1}^{n^+} c_{i\infty} = \sum_{i=n^++1}^{n} c_{i\infty} \equiv c_\infty \tag{S18}$$

where c_∞ is similar to the bulk concentration used for describing the diffusiophoresis in 1:1 binary electrolyte. In addition, c_∞ can be treated as ionic strength of multiple electrolyte system (*i.e.* $c_\infty = \sum c_{i\infty} / 2$). Substituting equation (S18) into equation (S17),

$$\rho_e = -2Fc_\infty \sinh\frac{F\psi}{RT}. \tag{S19}$$

In order to determine the diffusiophoretic velocity, equation (S19) was combined with the Stokes equation.

$$-\eta\nabla^2\mathbf{u} + \nabla p + \rho_e\nabla\psi = 0 \tag{S20}$$

where **u** and p are the flow velocity and the pressure, respectively. If $\lambda_D << a$ where a is the particle radius, the phoretic problem can be simplified to the osmotic problem as shown in Supplementary Figure 9(b) [8]. The boundary conditions were

$$u_x\big|_{y=0} = 0 \quad \text{and} \quad u_x\big|_{y\to\infty} = -U_P \tag{S21}$$

where u_x is the x-component of flow velocity, U_P is the phoretic speed and y-component of flow velocity (u_y) is assumed as 0. Since the electric potential gradient was neglected in equation (S16), U_P implied U_{CP}. The Stokes equation is linear so that $\mathbf{U}_{EP}$ can be determined by another formulation. In fact, the formulation from (S19) to (S21) was the same to the diffusiophoretic (or diffusioosmotic) problem in the case of 1:1 binary electrolyte [5]. Hence, in this work, we briefly discussed the mathematical derivations. The fact of $u_y = 0$ led the y-component of equation (S20) to

$$\frac{\partial p}{\partial y} - 2Fc_\infty \sinh\left(\frac{F\psi}{RT}\right)\frac{\partial\psi}{\partial y} = 0 \tag{S22}$$

and then

$$p - p_\infty = 2c_\infty RT\left[\cosh\left(\frac{F\psi}{RT}\right) - 1\right] \tag{S23}$$

where p_∞ is the pressure at the bulk. Combining equation (S23) with x-component of equation (S20),

$$\eta \frac{d^2 u_x}{dy^2} = 2RT\left[\cosh\left(\frac{F\psi}{RT}\right) - 1\right]\frac{dc_\infty}{dx}. \tag{S24}$$

In above, ψ can be determined by the Poisson-Boltzmann equation with appropriate boundary conditions.

$$\frac{d^2\psi}{dy^2} = \frac{2Fc_\infty}{\varepsilon}\sinh\left(\frac{F\psi}{RT}\right) \tag{S25}$$

and

$$\psi\big|_{y=0} = \zeta_p \quad \text{and} \quad \psi\big|_{y\to\infty} = 0. \tag{S26}$$

The analytical solution of the Poisson-Boltzmann equation was [5]

$$\tanh\left(\frac{F\psi}{4RT}\right) = \tanh\left(\frac{F\zeta_p}{4RT}\right)\exp(-\kappa y) \tag{S27}$$

where $\kappa^2 = 2F^2c_\infty / (\varepsilon RT)$. Thus, the solution of equation (S24) was

$$u_x\big|_{y\to\infty} - u_x\big|_{y=0} = \frac{2\varepsilon R^2T^2}{\eta F^2}\ln\left[1 - \tanh^2\left(\frac{F\zeta_p}{4RT}\right)\right]\frac{d\ln c_\infty}{dx}. \tag{S28}$$

Using boundary conditions of (S21),

$$U_{CP} = -\frac{2\varepsilon R^2T^2}{\eta F^2}\ln\left[1 - \tanh^2\left(\frac{F\zeta_p}{4RT}\right)\right]\frac{d\ln c_\infty}{dx}. \tag{S29}$$

Note that the formulation from equation (S19) to (S21) described the chemiphoretic problem so that U_P was replaced by U_{CP}. If the electrolyte is 1:1 binary solution, equation (S29) is the same with equation (S11).

The determination of $\mathbf{U}_{EP}$ was relatively simple. In the diffusiophoretic cell, there was no any current source or sink. This fact implied that the ionic current should be zero [9, 10]. Mathematically,

$$\mathbf{i} = F\sum_{i=1}^{n} z_i \mathbf{j}_i = 0 \tag{S30}$$

where $\mathbf{i}$ is the current density and $\mathbf{j}_i$ is the ionic flux of i-th species. In the far-field from the charged particle, equation (S30) became

$$\sum_{i=1}^{n}\left(-z_i D_i \nabla c_{i\infty} - \frac{z_i^{\,2} F D_i}{RT} c_{i\infty} \nabla \phi \right) = 0 \tag{S31}$$

where D_i is the diffusivity of i-th species and ϕ is the electric potential induced by salt-gradient. Rearranging above equation,

$$-\nabla \phi = \frac{RT}{F} \frac{\sum_{i=1}^{n} z_i D_i \nabla c_{i\infty}}{\sum_{i=1}^{n} z_i^{\,2} D_i c_{i\infty}} . \tag{S32}$$

This is the induced-electric field due to the difference of diffusion rate between dissolved ionic species. If $\lambda_D << a$, the Smoluchowski formula for electrophoresis holds. Thus,

$$\mathbf{U}_{EP} = \frac{\varepsilon \zeta_p}{\eta} \frac{RT}{F} \frac{\sum_{i=1}^{n} z_i D_i \nabla c_{i\infty}}{\sum_{i=1}^{n} z_i^{\,2} D_i c_{i\infty}} \tag{S33}$$

If the electrolyte is 1:1 binary solution, equation (S33) is the same with equation (S12). Conclusively, the chemiphoretic and electrophoretic velocity around ion-exchange surface can be expressed by

$$\mathbf{U}_{CP} = -\frac{2\varepsilon R^2 T^2}{\eta F^2} \ln\left[1 - \tanh^2\left(\frac{F\zeta_p}{4RT} \right) \right] \nabla \ln\left(\frac{c_{Na} + c_{Cl} + c_H + c_{OH}}{2} \right) \tag{S34}$$

and

$$\mathbf{U}_{EP} = \frac{\varepsilon \zeta_p}{\eta} \frac{RT}{F} \frac{D_{Na} \nabla c_{Na} - D_{Cl} \nabla c_{Cl} + D_H \nabla c_H - D_{OH} \nabla c_{OH}}{D_{Na} c_{Na} + D_{Cl} c_{Cl} + D_H c_H + D_{OH} c_{OH}} . \tag{S35}$$

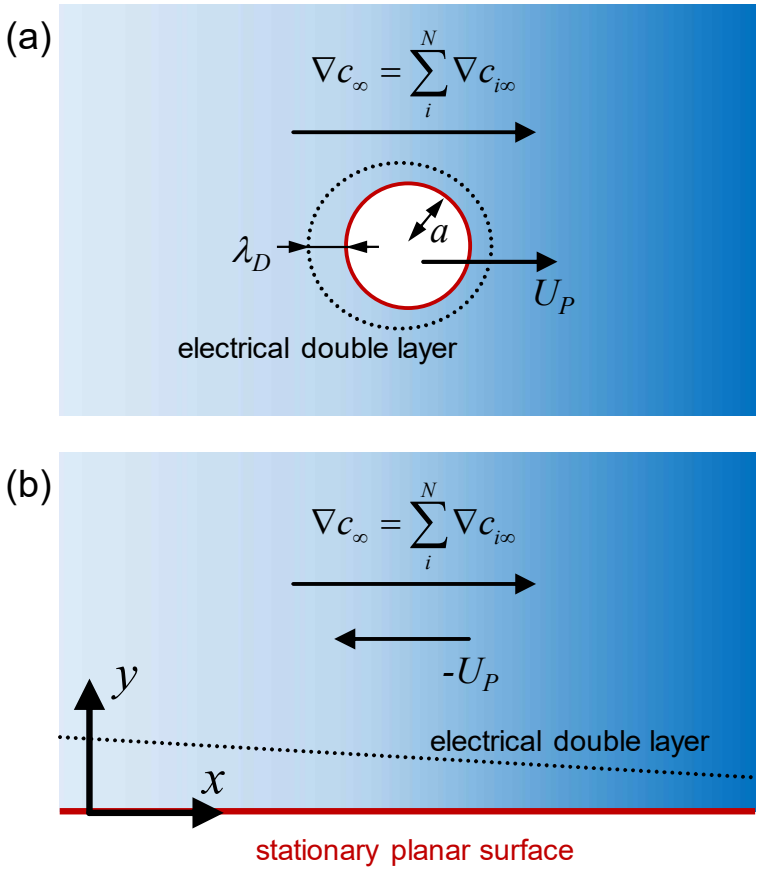

Supplementary Figure 9. Diffusiophoretic domain description. (a) A schematic representation for diffusiophoresis of spherical particle. If $\lambda_D << a$, the problem is equivalent to the case of (b).

References

1. J. Kim, I. Cho, H. Lee and S. J. Kim, *Scientific Reports*, 2017, **7**, 5091.
2. R. B. Schoch, J. Han and P. Renaud, *Reviews of Modern Physics*, 2008, **80**, 839-883.
3. J. L. Anderson, *Annual Review of Fluid Mechanics*, 1989, **21**, 61-99.
4. D. C. Prieve, *Advances in Colloid and Interface Science*, 1982, **16**, 321-335.
5. D. C. Prieve, J. L. Anderson, J. P. Ebel and M. E. Lowell, *Journal of Fluid Mechanics*, 1984, **148**, 247-269.
6. D. Velegol, A. Garg, R. Guha, A. Kar and M. Kumar, *Soft Matter*, 2016, **12**, 4686-4703.
7. W. Wang, W. Duan, S. Ahmed, T. E. Mallouk and A. Sen, *Nano Today*, 2013, **8**, 531-554.
8. J. H. Masliyah and S. Bhattacharjee, *Electrokinetic and Colloid Transport Phenomena*, Wiley, 2006.
9. R. A. Rica and M. Z. Bazant, *Physics of Fluids*, 2010, **22**, 112109.
10. T.-Y. Chiang and D. Velegol, *Journal of Colloid and Interface Science*, 2014, **424**, 120-123.